Theoretical design study on the electronic structure and photophysical properties of a series of osmium(II) complexes with different ancillary ligands

ARTICLE *in* POLYHEDRON · JANUARY 2015

Impact Factor: 2.01 · DOI: 10.1016/j.poly.2014.09.018

5 AUTHORS, INCLUDING:

Deming Han
Changchun University of Science and Tech…
30 PUBLICATIONS **97** CITATIONS

SEE PROFILE

Polyhedron 85 (2015) 506–510

Contents lists available at ScienceDirect

Polyhedron

journal homepage: www.elsevier.com/locate/poly

Theoretical design study on the electronic structure and photophysical properties of a series of osmium(II) complexes with different ancillary ligands

Deming Han [a], Jian Liu [a], Runzhong Miao [a], Lihui Zhao [a,*], Gang Zhang [b]

[a] School of Life Science and Technology, Changchun University of Science and Technology, Changchun 130022, PR China
[b] State Key Laboratory of Theoretical and Computational Chemistry, Institute of Theoretical Chemistry, Jilin University, Changchun 130023, PR China

ARTICLE INFO

Article history:
Received 29 June 2014
Accepted 7 September 2014

Keywords:
OLEDs
DFT
TDDFT
Phosphorescence
Osmium

ABSTRACT

The geometrical structures, electronic structures, absorption and phosphorescent properties of a series of osmium(II) complexes with the structure $(N^N)_2Os(P^P)$ [where N^N = 2-pyridyl phenyl triazolate, P^P = 1,2-bis(phospholano)methylene (**1**); 1,2-bis(phospholano)ethane (**2**); 1,2-bis(phospholano)-4-methyl-benzene (**3**); 1,2-bis(phospholano)benzene (**4**); 1,2-bis(phospholano)-4-cyano-benzene (**5**); 1,2-bis(phospholano)naphthalene (**6**)] have been investigated using density functional theory (DFT) and time-dependent density functional theory (TDDFT). Ionization potential and electron affinity values indicate that complex **5** has a good charge transfer balance to enhance device performance of organic light-emitting diodes (OLEDs). The lowest energy emissions of complexes **1**–**6** at the PBE0 level are localized at 663, 656, 660, 659, 647 and 656 nm, respectively. From the theoretical results, it can be predicted that complex **3** has possibly a larger k_r value than the other complexes. These theoretical studies could be useful in providing valuable information on the optical and electronic properties of phosphorescent materials used in organic light-emitting diodes (OLEDs).

1. Introduction

Over the past two decades, organic light-emitting diodes (OLEDs) have been an intriguing research field because of their potential applications in flat-panel displays and general solid-state lighting [1–5]. Recently, electroluminescent (EL) devices with phosphorescent metal–organic complexes of Ru(II), Os(II), Ir(III) and Pt(II) have been extensively synthesized and investigated [6–12]. In addition to complexes with Ir(III) as the central metal, many complexes based on Os(II) as the central metal were also considered as potential candidates for highly efficiency phosphorescent materials, which generally possess a shorter triplet-state exciton lifetime due to the enhancement of the heavy-metal atom participating in the lowest excited triplet manifolds [13–15]. For example, Tsang-Chi Lee et al. have reported a few new Os(II) complexes with the highly conjugated isoquiniolinyl triazolate chelate to obtain phosphors that shine at a longer wavelength region to develop efficient phosphorescent materials for OLED applications [2]. Much experimental and theoretical works have also been performed to obtain high efficiency Os(II)-based phosphorescent materials [16–22].

Recently, Lin and co-worker have synthesized a series of heteroleptic cyclometalated Os(II) complexes functionalized with 2-pyridyl (or 2-isoquinolyl) pyrazole chelates as the dopant for OLEDs [23]. Herein, to explore the influence of P^P ancillary ligands on the photophysical properties of Os(II) complexes, six Os(II) complexes (**1**–**6**) with the structure $(N^N)_2Os(P^P)$ [where N^N = 2-pyridyl phenyl triazolate, P^P = 1,2-bis(phospholano)methylene (**1**); 1,2-bis(phospholano)ethane (**2**); 1,2-bis(phospholano)-4-methyl-benzene (**3**); 1,2-bis(phospholano)benzene (**4**); 1,2-bis(phospholano)-4-cyano-benzene (**5**); 1,2-bis(phospholano)naphthalene (**6**)] have been investigated using density functional theory (DFT) and time-dependent density functional theory (TDDFT).

2. Computational details

The ground state geometry for each molecule was optimized by the density functional theory (DFT) method with the hybrid Hartree–Fock/density functional model (PBE0) based on Perdew–Burke–Erzenrhof (PBE) [24]. The geometry optimizations of the lowest triplet states (T_1) were performed by the PBE0 approach.

* Corresponding author. Tel.: +86 431 85583023.
E-mail address: zhaolihui@yahoo.com (L. Zhao).

http://dx.doi.org/10.1016/j.poly.2014.09.018
0277-5387/

On the basis of the ground and excited state equilibrium geometries, the time-dependent DFT (TDDFT) approach associated with the polarized continuum model (PCM) in dichloromethane (CH_2Cl_2) medium was applied to investigate the absorption and emission spectral properties. The LANL2DZ and 6-31G(d) basis sets were used for the Os atom and the other atoms, respectively. Furthermore, the stable configurations of these complexes can be confirmed by frequency analysis, in which no imaginary frequencies were found for all configurations at the energy minima. In addition, the positive and negative ions, with regard to "electron–hole" creation, are relevant to their use as OLED materials. Thus, the ionization potentials (IP), electron affinities (EA) and reorganization energies (λ) were obtained by comparing the energy levels of the neutral molecule with the positive ions and negative ions, respectively. The calculated electronic density plots for the frontier molecular orbitals were prepared using the GaussView 5.0.8 software. The simulated absorption spectra were obtained using the GaussSum 2.5 software [25]. All calculations were performed with the GAUSSIAN 09 software package [26].

3. Results and discussion

3.1. Geometries in the ground state S_0 and triplet excited state T_1

A sketch map of the six complexes **1**–**6** is presented in Fig. 1(a), and the optimized ground state geometric structure of complex **4** is shown in Fig. 1(b) along with the numbering of some key atoms. In addition, the main geometric parameters in the ground and lowest triplet states are summarized in Table S1 (Supplementary information).

All these heteroleptic Os(II) complexes **1**–**6** possess a distorted octahedral configuration with the 2-pyridyl phenyl triazolate and 1,2-bis(phospholano) group ligands. It can be seen that the metal–ligand bond distances amongst these complexes show slight changes. Especially, the selected bond distances for complexes **3** and **4** are very close, which indicates that the two complexes might have similar photophysical properties. Among the six complexes, the Os–P bond distances in complex **1** are longest, while the shortest ones are in complex **5**. The bond angles P1–Os–P2, P1–Os–N3, and P2–Os–N2 in complex **1** in the S_0 state are obviously smaller than those of the other five complexes. In addition, the dihedral angles P1–Os–N1–N2, P1–N1–N3–N4 and P2–N1–N2–N4 of complex **1** in the S_0 state are also larger than those of complexes **2**–**6**. Regarding the geometric parameters of all these complexes, there are some changes between the ground state (S_0) and the triplet excited state (T_1). For the triplet excited state T_1, the Os–N3, Os–N4, Os–P1 and Os–P2 bond distances are obviously longer compared with those in the S_0 state, while the Os–N1 and Os–N2 bond distances are evidently shorter. The P1–Os–P2 and N3–Os–N4 bond angles are slightly smaller on going from the S_0 to T_1 state. However, the N1–Os–-N2 and N1–Os–N4 bond angles have obviously increased (2–5°) on going from the S_0 to T_1 state. In addition, the P1–Os–N1–N2, P1–N1–N3–N4 and P2–N1–N2–N4 dihedral angles also show different changes between the S_0 and T_1 states.

3.2. Molecular orbital properties

The properties of the frontier molecular orbitals (FMOs), especially the HOMO (highest occupied molecular orbital) and LUMO (lowest unoccupied molecular orbital), have an important effect on the excited states and electronic transitions of organic light-emitting materials. The HOMO and LUMO distribution, energy levels and energy gaps between the LUMO and HOMO ($\Delta E_{L\rightarrow H}$) of complexes **1**–**6** have been plotted in Fig. 2. In addition, the

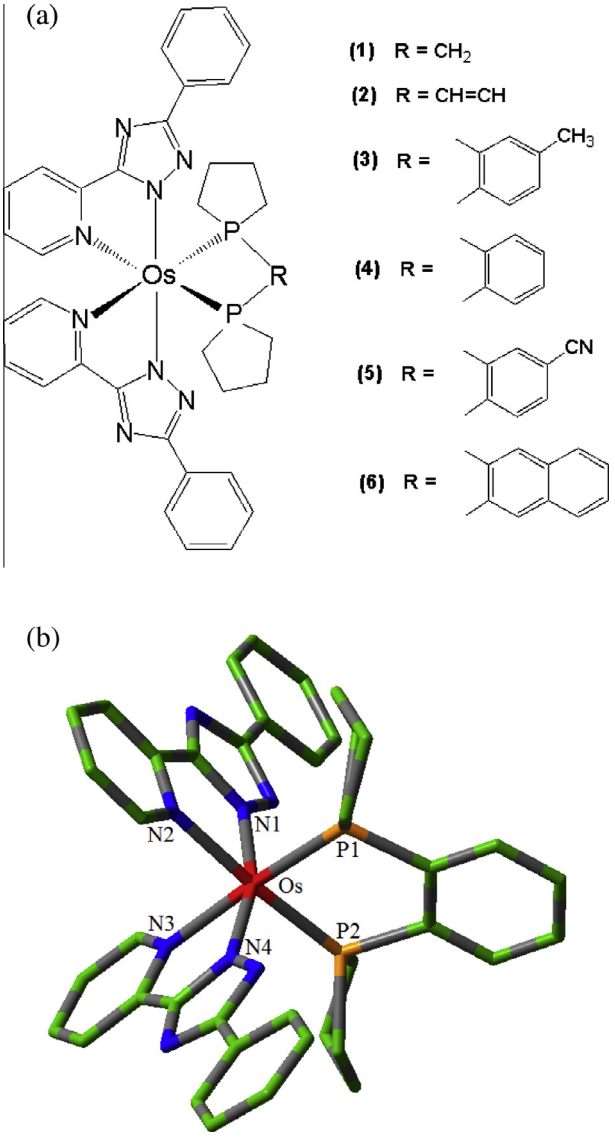

Fig. 1. (a) Sketch map of the structures of the osmium(II) complexes **1**–**6** (b) Representative optimized structure of **4** (H atoms omitted).

calculated FMOs compositions for **1**–**6** are also presented in Tables S2–S7 (Supplementary information).

From Fig. 2, it can be seen that complexes **1**–**4** have similar HOMO and LUMO energies level, with close $\Delta E_{L\rightarrow H}$ values (about 3.70 eV). This indicates that changing the P^P ancillary ligands for complexes **1**–**4** does not affect the energy levels of the HOMO and LUMO, or the energy gap. However, the HOMO and LUMO energies of complex **5** have obviously decreased in comparison with those of complexes **1**–**4**, with the lower $\Delta E_{L\rightarrow H}$ value (3.51 eV) being due to the electron-withdrawing group, CN, on the P^P ancillary ligand. In addition, complex **6** also has a small $\Delta E_{L\rightarrow H}$ value (3.55 eV). Fig. 2 and Tables S2–S7 show that the HOMOs for complexes **1**–**6** have a similar distribution of the Os d-orbital and N^N main ligand π-orbital. For example, the HOMO for complex **1** mainly resides on the Os 5d orbital (51%) and π(N^N) (46%). In addition, the LUMOs for complexes **1**–**4** show a similar distribution for the N^N ligand π*-orbital. However, the LUMOs of complexes **5** and **6** have mainly π*(P^P) compositions. This might suggest that the P^P ligands in complexes **5** and **6** play different roles in their photophysical properties. Additionally, it can be seen that the LUMOs of complexes **3** and **5** show an obvious difference due to the different substituent

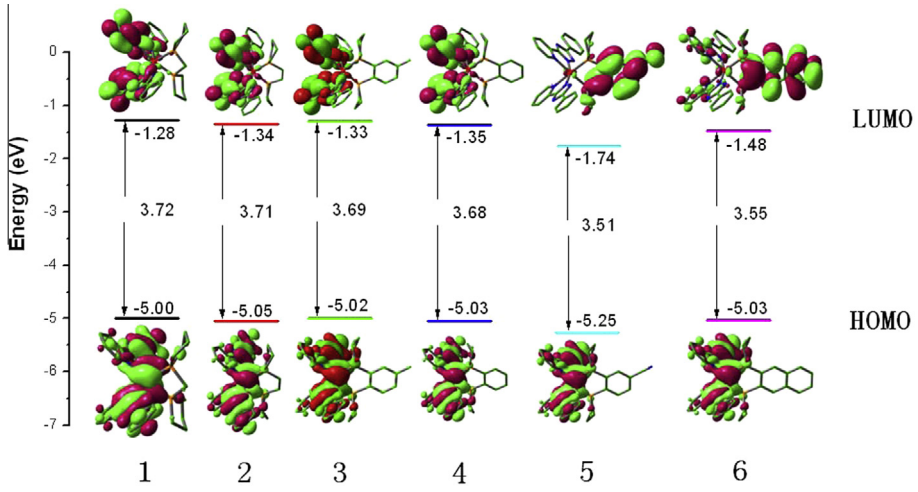

Fig. 2. Molecular orbital diagrams and HOMO and LUMO energies for complexes **1**–**6**.

groups, CH_3 (electron-donating) and CN (electron-withdrawing) on the 1,2-bis(phospholano) ligand.

3.3. Ionization potential (IP) and electronic affinity (EA)

The electroluminescent properties of these complexes as light-emitting layer materials in OLEDs are closely related to charge injection, transfer and balance as well as the exciton confinement in a device. Ionization potentials (IP), electron affinities (EA), reorganization energies (λ), hole and electron extraction potentials (HEP and EEP) have been calculated and are listed in Table 1. Detailed definitions for these physical quantities can be obtained from our previous work [27].

It is well-known that a larger EA (smaller IP) indicates easier injection of electrons (holes) into the emitting materials from the electron (hole) transporting layer. The IP values of complexes **3** and **6** are the smallest among complexes **1**–**6**, which indicates that the hole injection abilities are much stronger in complexes **3** and **6**. In addition, complex **5** has the largest EA value among complexes **1**–**6**, which means its ability to undergo electron injection is much easier than for the other complexes. The balance between the injection and transport of holes and electrons is important for emitting layer OLED materials. It is also known that λ is generally determined by fast changes in molecular geometry (internal reorganization energy λ_i) and by slow variations in the solvent polarization of the surrounding medium (the external reorganization energy λ_e). The contribution from λ_e can be neglected in OLED devices, the internal reorganization energy λ_i is the determinant factor. The reorganization energy can evaluate the charge transfer rate and balance. The λ_{hole} values for complexes **1**–**6** are larger than the $\lambda_{electron}$ values, which indicates that the electron transfer rate is better than the hole transfer rate. The energy difference between $\lambda_{electron}$ and λ_{hole} for complex **5** is the smallest among these complexes, resulting in good charge transfer balance and further enhancing device performance of OLEDs.

Table 1
The calculated vertical IP (IP_v), adiabatic IP (IP_a), hole extraction potential (HEP), vertical EA (EA_v) and adiabatic EA (EA_a), electron extraction potential (EEP) and reorganization energies for electron ($\lambda_{electron}$) and hole (λ_{hole}), unit: eV.

	IP_v	IP_a	HEP	EA_v	EA_a	EEP	$\lambda_{electron}$	λ_{hole}
1	5.848	5.624	5.429	0.237	0.337	0.431	0.194	0.419
2	5.920	5.710	5.499	0.300	0.403	0.506	0.206	0.421
3	5.844	5.620	5.411	0.307	0.407	0.5111	0.203	0.433
4	5.871	5.656	5.444	0.324	0.427	0.530	0.205	0.426
5	6.082	5.854	5.645	0.670	0.780	0.960	0.290	0.436
6	5.841	5.621	5.402	0.503	0.562	0.625	0.122	0.438

3.4. Absorption spectra

The absorption properties of complexes **1**–**6** were investigated using the TDDFT method on the basis of the optimized ground state geometries. The vertical electronic excitation energies, oscillator strengths (f), assignment and configurations are listed in Table S8 (Supplementary information). The UV–Vis absorption spectra in CH_2Cl_2 medium for these studied complexes are displayed in Fig. 3.

The lowest energy absorption wavelengths are located at 442 nm (f = 0.0145) for **1**, 437 nm (f = 0.0169) for **2**, 439 nm (f = 0.0161) for **3**, 438 nm (f = 0.0158) for **4**, 431 nm (f = 0.0142) for **5** and 438 nm (f = 0.0145) for **6**. It can be seen that the absorption peaks for these complexes are not obviously changed according to ancillary ligands. Fig. 3 shows that all these complexes have two obvious absorption peaks at about 240 and 295 nm, respectively. It can be seen that complex **5** has a stronger absorption at about 240 nm than the other complexes. From Table S8 and Fig. 2, it can also be seen that the lowest energy absorptions for complexes **1**–**4** are mainly attributed to the HOMO → LUMO transition with MLCT (singlet metal to ligand charge transfer)/ILCT (singlet intraligand charge transfer) character, described as a d(Os) + π(N^N) → π*(N^N) transition. However, complexes **5** and

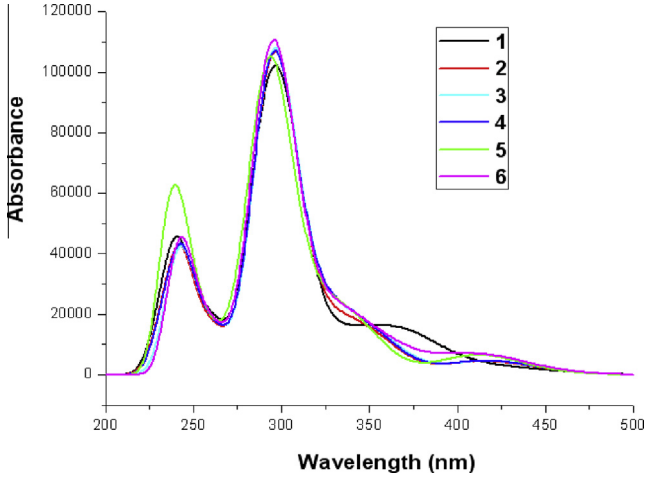

Fig. 3. Simulated absorption spectra in CH_2Cl_2 medium for complexes **1**–**6**.

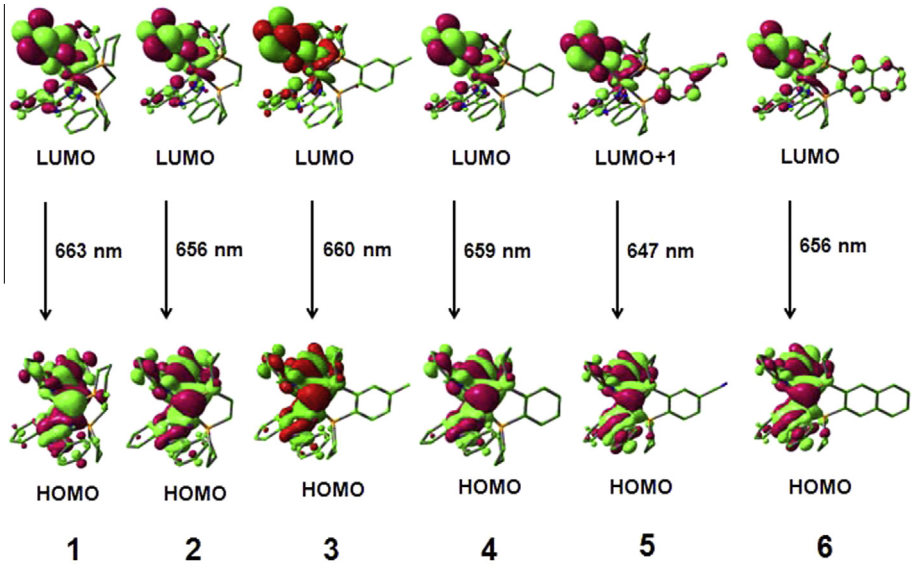

Fig. 4. Frontier molecular orbitals related to the emissions at 663, 656, 660, 659, 647 and 656 nm, respectively, for complexes **1**–**6**, simulated in CH_2Cl_2 medium at PBE0 level (H indicates HOMO, L indicates LUMO).

Table 2
Phosphorescent emissions of **1**–**6** in CH_2Cl_2 medium at the PBE0 level, along with the experimental wavelength (nm) available (H indicates HOMO, L indicates LUMO).

	λ (nm)/E(eV)	Configuration	Nature	Exptl.[a]
1	663/1.867	L → H(88%)	^{3}LMCT/^{3}LLCT/^{3}ILCT	
2	656/1.887	L → H(90%)	^{3}LMCT/^{3}LLCT/^{3}ILCT	
3	660/1.877	L → H(90%)	^{3}LMCT/^{3}LLCT/^{3}ILCT	
4	659/1.879	L → H(90%)	^{3}LMCT/^{3}LLCT/^{3}ILCT	634
5	647/1.913	L+1 → H(83%)	^{3}LMCT/^{3}LLCT/^{3}ILCT	
6	656/1.887	L → H(84%)	^{3}LMCT/^{3}LLCT/^{3}ILCT	

[a] From Ref. [23].

6 have different transitions, MLCT/LLCT (singlet ligand to ligand charge transfer). Additionally, the absorption intensities of complexes **5** and **6** near 300 nm are the strongest among the complexes studied, which would have a higher probability of intersystem crossing (ISC) from singlet to triplet states and accordingly an increase in the quantum yield for phosphorescence.

3.5. Phosphorescent properties

To check the computational method, six different density functionals (B3LYP, CAM-B3LYP, M05-2X, M06-2X, BP86 and PBE0) were used to calculate the emission properties of the synthesized complex **4** [28–30]. A good agreement with the experimental data was obtained for the PBE0 method, while an obvious disagreement was found for the other methods. Further, on the basis of the optimized T_1 structures, the emission wavelengths, emission energies and transition nature of complexes **1**–**6** were calculated with the PBE0 method in CH_2Cl_2 medium and the results are listed in Table 2. Frontier molecular orbitals related to emissions for complexes **1**–**6**, simulated in CH_2Cl_2 medium at the PBE0 level, have been displayed in Fig. 4. The partial compositions of the FMOs related to emission have also been presented in Table S9 (Supplementary information) to analyze the transition property of the emissions.

Table 3
The contribution of ^{3}MLCT (%) in the T_1 state and the energy gaps between the S_1 and T_1 states ($\Delta E_{S_1-T_1}$) (in eV), along with the transition electric dipole moment in the $S_0 \rightarrow S_1$ transition μ_{S_1}, the radiative decay rate k_r ($\times 10^5\ s^{-1}$) and non-radiative decay rate k_{nr} ($\times 10^5\ s^{-1}$), together with the measured lifetime τ [μs] and quantum yields Φ [%] for the studied complex **4** in CH_2Cl_2 medium.

	^{3}MLCT	$\Delta E_{S_1-T_1}$	μ_{S_1}	Φ[a]	τ[a]	k_r[a]	k_{nr}[a]
1	43.12	0.32	0.21				
2	41.40	0.38	0.24				
3	42.30	0.31	0.23				
4	42.30	0.37	0.22	0.49	1.52	3.20	3.40
5	35.69	0.38	0.20				
6	40.32	0.37	0.20				

[a] From Ref. [23].

The calculated lowest energy emissions for complexes **1**–**6** at the PBE0 level are localized at 663, 656, 660, 659, 647 and 656 nm, respectively. It can be seen that the lowest energy emission wavelength (659 nm) of complex **4** is in good agreement with the experimental data (634 nm) [23]. The transition characters of these lowest energy emissions for complexes **1**–**6** have L → H transition configurations, except for complex **5** with the L+1 → H transition. For complexes **1**–**5**, their emission transition characters are assigned to ^{3}LMCT (triplet ligand to metal charge transfer)/^{3}LLCT (triplet ligand to ligand charge transfer)/^{3}ILCT (triplet intraligand charge transfer) [π*(N^N) → d(Os) + π(N^N)]. Especially, complex **6** has the emission transition character [π*(N^N + P^P) → d(Os) + π(N^N)] due to the increase of the π-conjugation length from naphthalene substitution on the ancillary P^P ligands.

The emission quantum yield (Φ) can be affected by competition between k_r (radiative decay rate) and k_{nr} (non-radiative decay rate), i.e. $\Phi = k_r/(k_r + k_{nr})$. It can be seen that to increase the quantum yield, k_r should be increased and k_{nr} should be decreased, simultaneously or respectively [9,31]. In addition, k_r is also theoretically related to the mixing between S_1 and T_1, which is proportional to the spin–orbit coupling (SOC) and inversely proportional to the energy gap between the S_1 and T_1 states according to the following formula [32,33]:

$$k_r \approx \gamma \frac{\langle \psi_{S_1} | H_{S_0} | \psi_{T_1} \rangle^2 \mu_{S_1}^2}{(\Delta E_{S_1-T_1})^2} \quad (1)$$

$$\gamma = 16\pi^3 10^6 n^3 E_{em}^3 / 3h\varepsilon_0$$

where H_{S_0} is the Hamiltonian for the spin–orbit coupling, μ_{S_1} is the transition dipole moment in the $S_0 \rightarrow S_1$ transition, $\Delta E_{S_1-T_1}$ is the

energy gap between the S_1 and T_1 states, E_{em} represents the emission energy in cm^{-1} and n, h, and ε_0 are the refractive index, Planck's constant and the permittivity in a vacuum, respectively. Accordingly, the variation of quantum yield (Φ) can be qualitatively analyzed in theory from the above formula. Generally, the phosphorescence quantum efficiencies could be increased by a larger ^{3}MLCT composition and thus intersystem crossing (ISC). For the osmium atom, the direct involvement of the d(Os) orbital enhances the first-order SOC in the $T_1 \rightarrow S_0$ transition and thus the ISC, which would result in a drastic decrease of the radiative lifetime and avoid the non-radiative process [34]. The ^{3}MLCT contributions for complexes **1**–**6** are 43.12%, 41.40%, 42.30%, 42.30%, 35.69% and 40.32%, respectively (Table 3). The ^{3}MLCT contribution of **6** is smaller than those of the other complexes. It is also known that the phosphorescence quantum efficiencies are inversely proportional to $\Delta E_{S_1-T_1}$ [35]. A minimal $\Delta E_{S_1-T_1}$ value is good for enhancing the ISC rate, leading to a larger k_r value. The $\Delta E_{S_1-T_1}$ values for complexes **1**–**6** are also presented in Table 3, along with the μ_{S_1} values. The $\Delta E_{S_1-T_1}$ values are 0.32, 0.38, 0.31, 0.37, 0.38 and 0.37 eV for **1**–**6**, respectively. It is evident that the lower $\Delta E_{S_1-T_1}$ value, larger ^{3}MLCT contribution and higher μ_{S_1} value may account for a larger k_r, according to Eq. (1). From the data in Table 3, it can be seen that complex **3** has possibly a larger k_r value than the other complexes.

4. Conclusions

In this study the electronic structures and photophysical properties of six osmium(II) complexes (**1**–**6**) with the same 2-pyridyl phenyl triazolate main ligand and substituted 1,2-bis(phospholano) group ancillary ligands have been theoretically investigated. The ionization potentials and electron affinities have also been calculated to evaluate the injection abilities of holes and electrons into these complexes. It is obvious that complexes **1**–**4** have similar HOMO and LUMO energies level and close $\Delta E_{L\rightarrow H}$ values. The lowest energy absorption wavelengths for these complexes are slightly changed with the different ancillary ligands. The phosphorescent emissions properties of these complexes also show a lot of changes according to the substituted ancillary ligands. It is anticipated that the study could guide the further theoretical and experimental design of novel phosphorescent materials for use in OLEDs.

Acknowledgments

The authors are grateful for financial aid from the Program of Science and Technology Development Plan of Jilin Province (Grant Nos. 20140520090JH, 20130203032YY) and the Funds for Doctoral Scientific Research Startup of Changchun University of Science and Technology (Grant No. 40301855).

Appendix A. Supplementary data

Supplementary data associated with this article can be found, in the online version, at http://dx.doi.org/10.1016/j.poly.2014.09.018.

References

[1] M.S. Lowry, S. Bernhard, Chem. Eur. J. 12 (2006) 7970.
[2] T.C. Lee, J.Y. Hung, Y. Chi, Y.M. Cheng, G.H. Lee, P.T. Chou, C.C. Chen, C.H. Chang, C.C. Wu, Adv. Funct. Mater. 19 (2009) 2639.
[3] P. Schrogel, M. Hoping, W. Kowalsky, A. Hunze, G. Wagenblast, C. Lennartz, P. Strohriegl, Chem. Mater. 23 (2011) 4947.
[4] X.H. Shang, D.M. Han, D.F. Li, Z.J. Wu, Chem. Phys. Lett. 565 (2013) 12.
[5] Y. Seino, H. Sasabe, Y.J. Pu, J. Kido, Adv. Mater. 26 (2014) 1612.
[6] X.H. Shang, Y.Q. Liu, X.C. Qu, Z.J. Wu, J. Lumin. 143 (2013) 402.
[7] S. Welter, K. Brunner, J.W. Hofstraat, L. De Cola, Nature 421 (2003) 54.
[8] M.S. Lowry, W.R. Hudson Jr., R.A. Pascal, S. Bernhard, J. Am. Chem. Soc. 126 (2004) 14129.
[9] A.B. Tamayo, S. Garon, T. Sajoto, P.I. Djurovich, I.M. Tsyba, R. Bau, M.E. Thompson, Inorg. Chem. 44 (2005) 8723.
[10] S. Thomas III, K. Venkatesan, P. Müller, T.M. Swager, J. Am. Chem. Soc. 128 (2006) 16641.
[11] V.L. Whittle, J.A.G. Williams, Inorg. Chem. 47 (2008) 6596.
[12] R.D. Costa, F.J. Céspedes-Guirao, E. Ortí, H.J. Bolink, J. Gierschner, F. Fernández-Lázaro, A. Sastre-Santos, Chem. Commun. 26 (2009) 3886.
[13] X. Jiang, A.K.Y. Jen, B. Carlson, L.R. Dalton, Appl. Phys. Lett. 80 (2002) 713.
[14] X. Jiang, A.K.Y. Jen, B. Carlson, L.R. Dalton, Appl. Phys. Lett. 81 (2002) 3125.
[15] S. Lamansky, P. Djurovich, D. Murphy, F. Abdel-Razzaq, H.E. Lee, C. Adachi, P.E. Burrows, S.R. Forrest, M.E. Thompson, J. Am. Chem. Soc. 123 (2001) 4304.
[16] H.A. Nieuwenhuis, D.J. Stufkens, A. Vlcek, Inorg. Chem. 34 (1995) 3879.
[17] J. van Slageren, F. Hartl, D.J. Stufkens, Coord. Chem. Rev. 208 (2000) 309.
[18] J. van Slageren, A.L. Vermeer, D.J. Stufkens, M. Lutz, A.L.J. Spek, Organomet. Chem. 626 (2001) 118.
[19] S. Chardon-Noblat, A. Deronzier, F. Hartl, J. van Slageren, T. Mahabiersing, Eur. J. Inorg. Chem. 2001 (2001) 613.
[20] C.H. Chang, Y.H. Lin, C.C. Chen, C.K. Chang, C.C. Wu, L.S. Chen, W.W. Wu, Y. Chi, Org. Electron. 10 (2009) 1235.
[21] F.C. Hsu, Y.L. Tung, Y. Chi, C.C. Hsu, Y.M. Cheng, M.L. Ho, P.T. Chou, S.M. Peng, A.J. Carty, Inorg. Chem. 45 (2006) 10188.
[22] J.P. Zhang, X. Zhou, F.Q. Bai, H.X. Zhang, Acta Phys. -Chim. Sin. 24 (2008) 2243.
[23] C.H. Lin, C.W. Hsu, J.L. Liao, Y.M. Cheng, Y. Chi, T.Y. Lin, M.W. Chung, P.T. Chou, G.H. Lee, C.H. Chang, J. Mater. Chem. 22 (2012) 10684.
[24] C. Adamo, V. Barone, J. Chem. Phys. 110 (1999) 6158.
[25] N.M. O'Boyle, A.L. Tenderholt, K.M. Langner, J. Comput. Chem. 29 (2008) 839.
[26] M.J. Frisch, G.W. Trucks, H.B. Schlegel, G.E. Scuseria, M.A. Robb, J.R. Cheeseman, G. Scalmani, V. Barone, B. Mennucci, G.A. Petersson, H. Nakatsuji, M. Caricato, X. Li, H.P. Hratchian, A.F. Izmaylov, J. Bloino, G. Zheng, J.L. Sonnenberg, M. Hada, M. Ehara, K. Toyota, R. Fukuda, J. Hasegawa, M. Ishida, T. Nakajima, Y. Honda, O. Kitao, H. Nakai, T. Vreven, J.A. Montgomery Jr., J.E. Peralta, F. Ogliaro, M. Bearpark, J.J. Heyd, E. Brothers, K.N. Kudin, V.N. Staroverov, R. Kobayashi, J. Normand, K. Raghavachari, A. Rendell, J.C. Burant, S.S. Iyengar, J. Tomasi, M. Cossi, N. Rega, J.M. Millam, M. Klene, J.E. Knox, J.B. Cross, V. Bakken, C. Adamo, J. Jaramillo, R. Gomperts, R.E. Stratmann, O. Yazyev, A.J. Austin, R. Cammi, C. Pomelli, J.W. Ochterski, R.L. Martin, K. Morokuma, V.G. Zakrzewski, G.A. Voth, P. Salvador, J.J. Dannenberg, S. Dapprich, A.D. Daniels, J.B. Foresman, J.V. Ortiz, J. Cioslowski, D.J. Fox, GAUSSIAN 09, Gaussian Inc, Wallingford, CT, 2009.
[27] D.M. Han, G. Zhang, H.X. Cai, X.H. Zhang, L.H. Zhao, J. Lumin. 138 (2013) 223.
[28] T. Yanai, D. Tew, N. Handy, Chem. Phys. Lett. 393 (2004) 51.
[29] Y. Zhao, D.G. Truhlar, Theor. Chem. Acc. 120 (2008) 215.
[30] J.P. Perdew, Phys. Rev. B 33 (1986) 8822.
[31] S. Fantacci, F. De Angelis, A. Sgamellotti, A. Marrone, N. Re, J. Am. Chem. Soc. 127 (2005) 14144.
[32] S. Haneder, E.D. Como, J. Feldmann, J.M. Lupton, C. Lennartz, P. Erk, E. Fuchs, O. Molt, I. Münster, C. Schildknecht, G. Wagenblast, Adv. Mater. 20 (2008) 3325.
[33] N. Turro, Modern Molecular Photochemistry, University Science Books, Palo Alto, CA, 1991.
[34] C.H. Yang, Y.M. Cheng, Y. Chi, C.J. Hsu, F.C. Fang, K.T. Wong, P.T. Chou, C.H. Chang, M.H. Tsai, C.C. Wu, Angew. Chem., Int. Ed. 46 (2007) 2418.
[35] I. Avilov, P. Minoofar, J. Cornil, L. De Cola, J. Am. Chem. Soc. 129 (2007) 8247.